Investigation of the TP modeling possibilities of the Hovorka T1DM model

György Eigner*, István Böjthe†, Péter Pausits‡ and Levente Kovács*
*Research and Innovation Center of Óbuda University,
Physiological Controls Group, Óbuda University, Budapest, Hungary
Email: {eigner.gyorgy,kovacs.levente}@nik.uni-obuda.hu
†Budapest University of Technology and Economics, Budapest, Hungary
Email: bojthez@gmail.com
‡Research and Innovation Center of Óbuda University,
Antal Bejczy Center for Intelligent Robotics, Óbuda University, Budapest, Hungary
Email: peter.pausits@irob.uni-obuda.hu

***Abstract*—Controller design based on Linear Parameter Varying (LPV) and Linear Matrix Inequality (LMI) combination can be extremely useful in modeling and controller design for patient specific physiological systems, which are generally nonlinear, time varying systems. These methods allow us the usage of considerations which come from the linear controller design theorems, but require advanced mathematics and high computational capacity also. In this research we exhibit the usage of the Tensor Product (TP) model transformation regarding diabetes researches as a means to realize a Tensor Product based Type 1 Diabetes Mellitus model, whose basis is a control oriented, deviation based qLPV model.**

Our primary goal is to realize all possible TP models, derived by choosing different combination of parameters for the qLPV model, and to validate all of them, confirming that all the derived TP models approximately mimic the behavior of the original, nonlinear system having only numeric error.

Keywords: Type 1 Diabetes Mellitus, LPV model, TP model, Validation

I. Introduction

Given the availability of increased computational capacity, one "mainstream" direction of control theory focuses on the usage of design methodologies combining LPV- and LMI-based controllers. One of these is the TP kind modeling and control, whose ideology successfully matches the LPV and LMI disciplines, so much so that the realized TP models can be used directly in design based on LMI, and the TP model and TP controller are strongly connected via the calculated core tensor and convex weight functions. In this study, we focused on developing such a TP model, which is physiologically valid and approximates well the original nonlinear model. This is only the first, but necessary step on a longer research path, the next step being the realization of a TP based controller for the established TP model. This paper is structured as follows: first, we provide a summarized, necessary knowledge about the TP model transformation. After that, we present the used T1DM model and define the used parameters of it. Fourth, we show every possible qLPV models and the realized, matching TP models of them. After this, we demonstrate the validation for each of the realized TP models. Finally, we summarize the reached results and conclude our work.

Gy. Eigner was supported by the ÚNKP-16-3/IV. New National Excellence Program of the Ministry of Human Capacities. This project has received funding from the European Research Council (ERC) under the European Union's Horizon 2020 research and innovation programme (grant agreement No 679681).

II. Tensor Product Model Transformation of qLPV Models

The TP model transformation can grant the TP model functions of given functions [1], [2]. It is possible to use the TP model transformation in such a way that it provides us the TP type qLPV model because each qLPV model can be described with qLPV functions. [3]. The resulting TP model can accurately approximate the original qLPV model.

Definition 1 - qLPV model in SS form: Consider a qLPV model described in its SS representation, the compact form of it:

$$\begin{aligned}\dot{\mathbf{x}}(t) &= \mathbf{A}(\mathbf{p}(t))\mathbf{x}(t) + \mathbf{B}(\mathbf{p}(t))\mathbf{u}(t) + \mathbf{E}(\mathbf{p}(t))\mathbf{r}(t)\\ \mathbf{y}(t) &= \mathbf{C}(\mathbf{p}(t))\mathbf{x}(t) + \mathbf{D}(\mathbf{p}(t))\mathbf{u}(t) + \mathbf{D_2}(\mathbf{p}(t))\mathbf{u}(t)\end{aligned} \tag{1a}$$

$$\mathbf{S}(\mathbf{p}(t)) = \begin{pmatrix}\mathbf{A}(\mathbf{p}(t)) & \mathbf{B}(\mathbf{p}(t)) & \mathbf{E}(\mathbf{p}(t))\\ \mathbf{C}(\mathbf{p}(t)) & \mathbf{D}(\mathbf{p}(t)) & \mathbf{D_2}(\mathbf{p}(t))\end{pmatrix}, \tag{1b}$$

where $\mathbf{A}(\mathbf{p}(t)) \in \mathbb{R}^{k\times k}$ is the state matrix, $\mathbf{B}(\mathbf{p}(t)) \in \mathbb{R}^{k\times m}$ is the control input matrix, $\mathbf{E}(\mathbf{p}(t)) \in \mathbb{R}^{k\times h}$ is the disturbance input matrix, $\mathbf{C}(\mathbf{p}(t)) \in \mathbb{R}^{l\times k}$ is the output matrix, $\mathbf{D}(\mathbf{p}(t)) \in \mathbb{R}^{l\times m}$ is the control input forward matrix and $\mathbf{D_2}(\mathbf{p}(t)) \in \mathbb{R}^{l\times h}$ disturbance input forward matrix. Additionally, $\mathbf{u}(t) \in \mathbb{R}^m$, $\mathbf{r}(t) \in \mathbb{R}^h$, $\mathbf{y}(t) \in \mathbb{R}^l$ and $\mathbf{x}(t) \in \mathbb{R}^k$ vectors are the control and disturbance inputs, output and state vector, respectively. $\mathbf{S}(\mathbf{p}(t)) \in \mathbb{R}^{(k+l)\times(k+m+h)}$ is the parameter dependent system matrix, which equivocally determines the qLPV system. Furthermore, the $\mathbf{p}(t) \in \Omega \in \mathbb{R}^N$ is the time dependent parameter vector.

Definition 2 - Transformational space Ω: the confined (closed) N dimensional hyperspace (hypercube), which is

determined by the minimum and maximum values of the scheduling parameters, as the elements of the parameter vector $p(t)$: $\Omega = [p_{1,min}, p_{1,max}] \times [p_{2,min}, p_{2,max}] \times ... \times [p_{N,min}, p_{N,max}] \in \mathbb{R}^N$.

Definition 3 - Finite element convex polytopic model: it describes the actual model $\mathbf{S}(t)$ as the convex combination of the $\mathbf{S}_r \in \mathbb{R}^{(k+l)\times(k+m+h)}$ LTI vertex system inside the Ω ($p(t) \in \Omega$):

$$\mathbf{S}(\mathbf{p}(t)) = \sum_{r=1}^{R} w_r(p(t))\mathbf{S}_r \ , \tag{2}$$

where the convexity requires that $w_r(p(t)) \in [0,1]$ and R are confined.

Definition 4 - A TP type convex polytopic model with finite elements : describing the actual model $\mathbf{S}(t)$ as the convex combination of the $\mathbf{S}_r \in \mathbb{R}^{(k+l)\times(k+m+h)}$ LTI vertex system inside the Ω ($p(t) \in \Omega$):

$$\mathbf{S}(\mathbf{p}(t)) = \sum_{i_1=1}^{I_1}\sum_{i_2=1}^{I_2}...\sum_{i_N=1}^{I_N}\prod_{n=1}^{N} w_{n,i_n}(p_n(t))\mathbf{S}_{i_1,i_2,...,i_N} \ . \tag{3}$$

The compact notation of (3) based on [3]:

$$\mathbf{S}(\mathbf{p}(t)) = \mathcal{S} \overset{\mathrm{N}}{\underset{\mathrm{n=1}}{\boxtimes}} \mathbf{w}_n(p_n(t)) \ , \tag{4}$$

where the coefficient tensor $\mathcal{S} \in \mathbb{R}^{I_1\times I_2\times...\times I_N\times(k+l)\times(k+m)}$ is derived from the $\mathbf{S}_{i_1,i_2,...,i_N}$ LTI vertex system and the row vector $\mathbf{w}_n(p_n(t))$ consists of $w_{n,i_n}(p_n(t))$ $(i_n = 1...I_N)$ continuous weighting functions having a single variable.

Definition 5 - The TP model transformation: given a qLPV model of (1a) the TP model transformation grants us an effective numerical method that transforms given model into a TP model form of (4). This way, several LMI based controller design methodologies can be applied directly on the given TP model. The TP model transformation also allows the use of convex hull manipulation amid the transformation. The number of used LTI vertexes and the properties of the applied HOSVD process and the used TP function influence the accuracy of the resulting TP model. Detailed description with examples can be found in [3].

Definition 6 - The canonical form of qLPV models based on HOSVD method: without the manipulation of the convex hull and the reduction in complexity, the result of the TP model transformation is the numerical reconstruction of the given qLPV model. Here, because of the HOSVD is used on qLPV models (matrix functions), the resulting HOSVD canonical form consists of singular functions in orthonormal structure and a core tensor, which contains system vertices assigned to the higher order singular values. For further details and description see [3], [4].

Definition 7 - Convex TP model: a model resulting after TP transformation is convex, if the following criteria regarding the weighting functions are satisfied:

$$\begin{aligned} &\forall n, i, p_n(t) : w_{n,i_n}(p_n(t)) \in [0,1] \\ &\forall n, p_n(t) : \sum_{i=1}^{I_n} w_{n,i_n}(p_n(t)) = 1 \end{aligned} \ . \tag{5}$$

Depending on the type of the application (qLPV model) and the required properties, several convex hulls can be applied on the parameter space [3]. The Minimal Volume Simplex (MVS) type hull is a tight convex hull – includes only that volume wherein the system can be found during operation –, which is applied in this study.

Definition 8 - MVS-type convex TP model: the following TP model

$$\mathbf{S}(\mathbf{p}) = \mathcal{S} \overset{\mathrm{N}}{\underset{\mathrm{n=1}}{\boxtimes}} \mathbf{w}^{(n)}(p_n) \ , \tag{6}$$

is a MVS-type convex model, if the $(\mathcal{S})_{j_n=j}$ n-mode subtensors develop a minimal volume bounding simplex for $\mathcal{S} \times_n \mathbf{w}_{j_n}^{(n)}(p_n)$ trajectory over $n = 1..N$ for the $\mathcal{S} \in \mathbb{S}^{J_1\times...\times J_N}$ core tensor, which is realized from the $\mathbf{S}_{j_1,...,j_N}$ matrices.Additional derivations, explanations and case studies can be found in [3], [5]–[9]. We this study we utilized the TP Toolbox®. The toolbox is a MATLAB based tool and is a means to a convenient and effective possibility to realize the TP based approached. The TP toolbox is available under [10].

III. T1DM MODEL

In this study we used a modified version of the Hovorka-model, which is a well known and widely used higher order T1DM model originally developed by Hovorka et al in [11] and modified by Naerum in [12]. The equations of the model are the following:

$$\dot{D}_1(t) = A_G D(t) - \frac{D_1(t)}{\tau_D} \ , \tag{7a}$$

$$\dot{D}_2(t) = \frac{D_1(t)}{\tau_D} - \frac{D_2(t)}{\tau_D} \ , \tag{7b}$$

$$\dot{S}_1(t) = u(t) - \frac{S_1(t)}{\tau_S} \ , \tag{7c}$$

$$\dot{S}_2(t) = \frac{S_1(t)}{\tau_S} - \frac{S_2(t)}{\tau_S} \ , \tag{7d}$$

$$\begin{aligned} \dot{Q}_1(t) = \frac{D_2(t)}{\tau_D} - F_{01,c} - F_R(t) - x_1(t)Q_1(t) \\ +k_{12}Q_2(t) + EGP_0(1 - x_3(t)) \end{aligned} \ , \tag{7e}$$

$$\dot{Q}_2(t) = x_1(t)Q_1(t) - (k_{12} + x_2(t))Q_2(t) \ , \tag{7f}$$

$$\dot{I}(t) = \frac{S_2(t)}{\tau_S V_I} - k_e I(t) \ , \tag{7g}$$

$$\dot{x}_1(t) = -k_{a1}x_1(t) + k_{b1}I(t) \ , \tag{7h}$$

$$\dot{x}_2(t) = -k_{a2}x_2(t) + k_{b2}I(t) \ , \tag{7i}$$

$$\dot{x}_3(t) = -k_{a3}x_3(t) + k_{b3}I(t) \ . \tag{7j}$$

The model consist of four main submodels, assigned to the state variables. The CHO absorption submodel (D_1, D_2 states measured in mmol) represents the glucose absorption; the nonlinear glucose-insulin core model (Q_1, Q_2 states measured in mmol) describes the glucose-insulin dynamics and cross effects; the insulin absorption submodel (S_1, S_2 states measured in mU) realizes the subcutaneous insulin absorption and the insulin kinematic submodel (I, x_{1-3} states) represents the insulinaemia and insulin effects. $d(t)$ g/min and $u(t)$ mU/min are the CHO and insulin intakes, respectively. The equations are completed with other functions, as well:

$$D(t) = \frac{1000 \cdot d(t)}{M_{wG}} \ , \tag{8a}$$

$$G(t) = \frac{Q_1(t)}{V_G} \ , \tag{8b}$$

$$F_R = \begin{cases} 0.003(G(t)-9)V_G & G(t) \geq 9mmol/L \\ 0 & \text{otherwise} \end{cases} \ , \tag{8c}$$

$$F_{01,c} = \begin{cases} F_{01} & G(t) \geq 4.5mmol/L \\ \dfrac{F_{01}G(t)}{4.5} & \text{otherwise} \end{cases} \ , \tag{8d}$$

where $D(t)$ is the CHO input in mmol/min, $G(t)$ is the output of the model and $F_{01,c}, F_R$ are the output related saturations (nonlinearities).

In this study we used the following parameter set: BW = 70 kg, M_{wG} = 180.15588 g/mol, k_{12} = 0.066 1/min, k_{a1} = 0.006 1/min, k_{a2} = 0.06 1/min, k_{a3} = 0.03 1/min, k_e = 0.138 1/min, τ_D = 40 min, τ_S = 55 min, A_G = 0.8, V_I/BW = 0.12 L/kg, V_I/BW = 0.16 L/kg, EGP_0/BW = 0.0161 $Lkg^{-1}min^{-1}$, F_{01}/BW = 0.00097 $Lkg^{-1}min^{-1}$, S_{IT} = 51.2 10^{-4} L/mU, S_{ID} = 8.2 10^{-4} L/mU, S_{IE} = 520 10^{-4} L/mU. Exact description of the meaning of the parameters can be found in [11], [12].

IV. DERIVATION OF THE POSSIBLE QLPV MODELS

A. GENERAL CONSIDERATIONS

Definition 9 - The qLPV model function: a given, parameter dependent qLPV model is determined by its compact form presented in (1b). This qLPV model form can be directly used in regards to the TP model transformation.

Definition 10 - Control oriented, deviation based qLPV model: these kind of qLPV models depict the state differences, that is relative to the target equilibrium: $\Delta x(t) = x(t) - x_{equilibrium}$. Furthermore, such kind of qLPV models are able to portray the error dynamics of the given qLPV model and this dynamics relates to the deviation of the states of the model from the given model equilibrium: $\Delta\dot{x}(t) = \dot{x}(t) - \dot{x}_{equilibrium} = \dot{x}(t) - 0$. Here, $x(t)$ is the state vector, $\Delta x(t)$ is the state deviation from the $x_{equilibrium}$, where the latter is the desired operating state vector. The goal of the control here is to eliminate the deviation (state error) over time.

B. qLPV MODEL OF THE USED T1DM MODEL

In this section, we derived each of the possible qLPV models from the original Hovorka model, which can serve as basis for our later investigations regarding to controller design. Since, there are several possible model equilibriums and the mathematical tools allow several algebraic transformations, more than one viable qLPV model exists. It should be noted that only those state equations that contain nonlinearity (7e)-(7f) have more than one possible transformed form and each of the other equations have only one possible transformation. According to the previous general considerations sub-chapter, firstly, the investigation of the possible steady states is required.

Notation 1 - We consequently use the short x_d term instead the long $x_{equilibrium}$ in order to mark the state equilibrium in the latter part of the article.

C. STEADY STATES CALCULATIONS

We started from the following consideration: if, the $Q_{1,d}$ and u_d are acknowledged as known, each steady state value of the states can be determined by the rearrangement of the model equations. Basically, if Q_{1d} and u_d are given, the steady states (equilibriums) are:

$$\begin{matrix} S_{1d} = u_d\tau_S \\ S_{2d} = S_{1d} \end{matrix} \ , \tag{9a}$$

$$I_d = \frac{1}{\tau_S V_I k_e} S_{2d} \ , \tag{9b}$$

$$x_{1d} = k_{b1}/k_{a1} I_d \ , \tag{9c}$$

$$x_{2d} = k_{b2}/k_{a2} I_d \ , \tag{9d}$$

$$x_{3d} = k_{b3}/k_{a3} I_d \ , \tag{9e}$$

$$Q_{2d} = x_{1d}Q_{1d}/(k_{12} + x_{2d}) \ , \tag{9f}$$

$$\begin{matrix} D_{2d} = (F_{01,c,d} + FR_d + x_{1d}Q_{1d} - k_{12}Q_{2d} - \\ EGP_0(1 + x_{3d})) \\ D_{1d} = D_{2d} \end{matrix} \ , \tag{9g}$$

$$d_d = D_{1d}M_{wG}/(1000A_G\tau_D) \ . \tag{9h}$$

D. qLPV MODEL DERIVATION

Subsequently, we will follow the following steps: i) - demonstration of the transformation on one state; ii) - description each transformed states, which only have one possible transformed form; iii) - investigation of the "critical states". For the algebraic transformation of (7a), we used the direct substitution of (8a), as well:

$$\begin{matrix} \Delta\dot{D}_1(t) = \dot{D}_1(t) - 0 = \\ = \dfrac{1000A_G}{MwG} d(t) - \dfrac{1}{\tau_D} D_1(t) - \\ \left[\dfrac{1000A_G}{MwG} \Delta d_d - \dfrac{1}{\tau_D} D_{1d} \right] = \\ \dfrac{1000A_G}{MwG}(d(t) - d_d) - \dfrac{1}{\tau_D}(D_1(t) - D_{1d}) \\ \Delta\dot{D}_1(t) = \dfrac{1000A_G}{MwG}\Delta d(t) - \dfrac{1}{\tau_D}\Delta D_1(t) \end{matrix} \ . \tag{10}$$

We derived the resulting state variables similar to (10), except Q_1 and Q_2:

$$\Delta\dot{D}_2(t) = \frac{1}{\tau_D}\Delta D_1(t) - \frac{1}{\tau_D}\Delta D_2(t) \ . \tag{11}$$

$$\Delta\dot{S}_1(t) = \Delta u(t) - \frac{1}{\tau_S}\Delta S_1(t) \ . \tag{12}$$

$$\Delta\dot{S}_2(t) = \frac{1}{\tau_S}\Delta S_1(t) - \frac{1}{\tau_S}\Delta S_2(t) \ . \tag{13}$$

$$\Delta\dot{I}(t) = \frac{1}{\tau_S V_I}\Delta S_2(t) - k_e\Delta I(t) \ . \tag{14}$$

$$\Delta\dot{x}_1(t) = -k_{a1}\Delta x_1(t) + k_{b1}\Delta I(t) \ . \tag{15}$$

$$\Delta\dot{x}_2(t) = -k_{a2}\Delta x_2(t) + k_{b2}\Delta I(t) \ . \tag{16}$$

$$\Delta\dot{x}_3(t) = -k_{a3}\Delta x_3(t) + k_{b3}\Delta I(t) \ . \tag{17}$$

In case of Q_1 and Q_2, more than one nonlinearity causing terms need to be considered: the numerous multiplication of time functions and the ramp type saturations belong to $F_{01,c}$ and F_R. The two saturations can be merged into one term, if we use directly the term $G(t) = Q_1(t)/V_G$ from (8b), as follows:

$$\Delta F(Q_1) = F(Q_1) - F(Q_{1,d}) = \\ = \begin{cases} 0.003\left(\frac{Q_1}{V_G} - 9\right)V_G & \text{if} \quad 9 \le \frac{Q_1(t)}{V_G} \\ 0 & \text{if} \quad 4.5 \le \frac{Q_1(t)}{V_G} < 9 \\ F_{01}\left(\frac{Q_1}{4.5V_G} - 1\right) & \text{if} \quad \frac{Q_1(t)}{V_G} < 4.5 \end{cases} . \tag{18}$$

Essentially, $\Delta Q_1(t)$ will not be zero at any time. Hence, the limits of the saturation guarantees that the involvement of $\Delta Q_1(t)$ term into the (17) as a multiplication by 1 cannot cause critical singularity at any time, so:

$$\frac{\Delta F(Q_1)}{\Delta Q_1(t)}\Delta Q_1(t) = \\ = \begin{cases} \frac{0.003\left(\frac{Q_1}{V_G} - 9\right)V_G}{\Delta Q_1(t)}\Delta Q_1(t) & \text{if} \quad 9 \le \frac{Q_1(t)}{V_G} \\ \frac{0}{\Delta Q_1(t)}\Delta Q_1(t) & \text{if} \quad 4.5 \le \frac{Q_1(t)}{V_G} < 9 \\ \frac{F_{01}\left(\frac{Q_1}{4.5V_G} - 1\right)}{\Delta Q_1(t)}\Delta Q_1(t) & \text{if} \quad \frac{Q_1(t)}{V_G} < 4.5 \end{cases} , \tag{19}$$

term can be used in order to associate the saturation to the $\Delta Q_1(t)$ state, which makes the accurate mathematical transformation achievable. It should be noted that more than one possible transformed form can be derived from (7e) and (7f).

Nevertheless, that one is the most useful, where the parameter vector is $p = [Q_1(t), Q_2(t)]^T$, which means, only the $Q_1(t)$ and $Q_2(t)$ states (BG related states) are the scheduling variables. However, the goal of this paper is to confirm, that it does not matter what we choose as parameters for the qLPV model, all of them will approximately mimic the behavior of the original system and the realized TP models can be used in our further research. $\Delta\dot{Q}_1(t)$ can be expressed in two ways, the parameter being either $Q_1(t)$ or $x_1(t)$:

$$\Delta\dot{Q}_1(t) = \frac{\Delta D_2(t)}{\tau_D V_G} - \frac{\Delta F(Q_1)}{\Delta Q_1(t)}\Delta Q_1(t) + k_{12}\Delta Q_2(t) \\ -EGP_0\Delta x_3(t) - x_{1d}\Delta Q_1(t) - Q_1(t)\Delta x_1(t) \tag{20a}$$

$$\Delta\dot{Q}_1(t) = \frac{\Delta D_2(t)}{\tau_D V_G} - \frac{\Delta F(Q_1)}{\Delta Q_1(t)}\Delta Q_1(t) + k_{12}\Delta Q_2(t) \\ -EGP_0\Delta x_3(t) - x_1(t)\Delta Q_1(t) - Q_{1d}\Delta x_1(t) \tag{20b}$$

Similar to this, $\Delta\dot{Q}_2(t)$ can be expressed in four ways, where chosen parameters are: $\mathbf{p}(t) = [x_1(t), x_2(t)]^T$ in case of (21a); $\mathbf{p}(t) = [x_1(t), Q_2(t)]^T$ in case of (21b), $\mathbf{p}(t) = [Q_1(t), x_2(t)]^T$ in case of (21c) or $\mathbf{p}(t) = [Q_1(t), Q_2(t)]^T$ in case of (21d).

$$\Delta\dot{Q}_2(t) = -k_{12}\Delta Q_2(t) + x_1(t)\Delta Q_1(t) + \\ Q_{1d}\Delta x_1(t) - x_2(t)\Delta Q_2(t) - Q_{2d}\Delta x_2(t) \tag{21a}$$

$$\Delta\dot{Q}_2(t) = -k_{12}\Delta Q_2(t) + x_1(t)\Delta Q_1(t) + \\ Q_{1d}\Delta x_1(t) - x_{2d}\Delta Q_2(t) - Q_2(t)\Delta x_2(t) \tag{21b}$$

$$\Delta\dot{Q}_2(t) = -k_{12}\Delta Q_2(t) + x_{1d}\Delta Q_1(t) + \\ Q_1(t)\Delta x_1(t) - x_2(t)\Delta Q_2(t) - Q_{2d}\Delta x_2(t) \tag{21c}$$

$$\Delta\dot{Q}_2(t) = -k_{12}\Delta Q_2(t) + x_{1d}\Delta Q_1(t) + \\ Q_1(t)\Delta x_1(t) - x_{2d}\Delta Q_2(t) - Q_2(t)\Delta x_2(t) \tag{21d}$$

As mentioned before, $Q_1(t)$ must be part of the $\mathbf{p}(t)$ parameter vector because the saturation guarantees, that singularity can not occur. Six $\mathbf{p}(t)$ parameter vectors can be assigned, resulting in six different models:

- $\mathbf{p}_1 = [Q_1(t), Q_2(t)]^T$ using (20a) and (21d), $T_1 = x_{1d}, T_2 = x_{1d}, T_3 = -(k_{12} + x_{2d}), T_4 = -Q_1(t), T_5 = Q_1(t), T_6 = -Q_2(t)$
- $\mathbf{p}_2 = [Q_1(t), x_2(t)]^T$ using (20a) and (21c), $T_1 = x_{1d}, T_2 = x_{1d}, T_3 = -(k_{12} + x_2(t)), T_4 = -Q_1(t), T_5 = Q_1(t), T_6 = -Q_{2d}$
- $\mathbf{p}_3 = [Q_1(t), Q_2(t), x_1(t)]^T$ using (20a) and (21b), $T_1 = x_{1d}, T_2 = x_1(t), T_3 = -(k_{12} + x_{2d}), T_4 = -Q_1(t), T_5 = Q_{1d}, T_6 = Q_2(t)$
- $\mathbf{p}_4 = [Q_1(t), Q_2(t), x_1(t)]^T$ using (20b) and (21d), $T_1 = x_1(t), T_2 = x_{1d}, T_3 = -(k_{12} + x_{2d}), T_4 = -Q_{1d}, T_5 = Q_1(t), T_6 = -Q_2(t)$
- $\mathbf{p}_5 = [Q_1(t), x_1(t), x_2(t)]^T$ using (20a) and (21a), $T_1 = x_{1d}, T_2 = x_1(t), T_3 = -(k_{12} + x_2(t), T_4 = -Q_1(t), T_5 = Q_{1d}, T_6 = -Q_{2d}$
- $\mathbf{p}_6 = [Q_1(t), x_1(t), x_2(t)]^T$ using (20b) and (21d), $T_1 = x_1(t), T_2 = x_{1d}, T_3 = -(k_{12} + x_{2d}), T_4 = -Q_{1d}, T_5 = Q_1(t), T_6 = -Q_2(t)$

$\mathbf{T} = [T_1, T_2, T_3, T_4, T_5, T_6]$ is a vector representing the changes that occur in the state space on specific spots, as displayed on (22). The six assembled models differ from

each other based on which equations we choose to describe ΔQ_1 and ΔQ_2. We used the qLPV model in form of (1b), the derived equations (10)-(19), if the state variables are $\Delta\mathbf{x} = [\Delta D_1, \Delta D_2, \Delta Q_1, \Delta Q_2, \Delta S_1, \Delta S_2, \Delta I, \Delta x_1, \Delta x_2, \Delta x_3]^T$.

V. TP MODEL

After the derivation of the proper qLPV models in convenient state space form (22), TP model transformation can be executed on them. This process was also done six times with different state space forms. The definitions in Sec. II describe the details of the process of TP model transformation, however, further details, with examples can be found in [3], [5]–[7]. Broadly, the $\mathbf{p}(t)$ dependent qLPV model of 22 were sampled over the domains of $Q_1(t)$ and $Q_2(t)$ between 34..185 mmol with 151 grid points at each dimensions. The sampling domain for $x_1(t)$ and $x_2(t)$ was 0...55 with each having 55 grid points at each dimensions. The application of the compact HOSVD algorithm [3] provided the compact $\mathcal{S}$ core tensor and the MVS-type weighting functions - which can be seen on Figs. 1–3 – were used to realize the TP model in the form of (6). In this way, the occurred TP models can be expressed by one of the following, depending on the $\mathbf{p}(t)$ parameter vector:

$$\text{for } \mathbf{p}_1 : \mathbf{S}(Q_1(t), Q_2(t)) = \mathcal{S} \overset{2}{\underset{n=1}{\boxtimes}} \mathbf{w}^{(n)}(\mathbf{p}_n) = \mathcal{S} \times_1 \mathbf{w}_1(Q_1(t)) \times_2 \mathbf{w}_2(Q_2(t)) \quad . \tag{23a}$$

$$\text{for } \mathbf{p}_2 : \mathbf{S}(Q_1(t), x_2(t)) = \mathcal{S} \overset{2}{\underset{n=1}{\boxtimes}} \mathbf{w}^{(n)}(\mathbf{p}_n) = \mathcal{S} \times_1 \mathbf{w}_1(Q_1(t)) \times_2 \mathbf{w}_2(x_2(t)) \quad . \tag{23b}$$

$$\text{for } \mathbf{p}_3 \text{ and } \mathbf{p}_4 : \mathbf{S}(Q_1(t), Q_2(t), x_1(t)) = \mathcal{S} \overset{3}{\underset{n=1}{\boxtimes}} \mathbf{w}^{(n)}(\mathbf{p}_n) = \mathcal{S} \times_1 \mathbf{w}_1(Q_1(t)) \times_2 \mathbf{w}_2(Q_2(t)) \times_3 \mathbf{w}_2(x_1(t)) \quad . \tag{23c}$$

$$\text{for } \mathbf{p}_5 \text{ and } \mathbf{p}_6 : \mathbf{S}(Q_1(t), x_1(t), x_2(t)) = \mathcal{S} \overset{3}{\underset{n=1}{\boxtimes}} \mathbf{w}^{(n)}(\mathbf{p}_n) = \mathcal{S} \times_1 \mathbf{w}_1(Q_1(t)) \times_2 \mathbf{w}_2(x_1(t)) \times_3 \mathbf{w}_2(x_2(t)) \quad . \tag{23d}$$

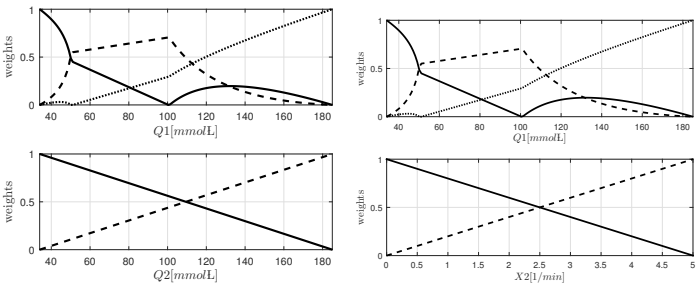

(a) $\mathbf{w}(\mathbf{p}_1)$ (b) $\mathbf{w}(\mathbf{p}_2)$

Figure 1: Weighting functions belong to (23a) (left) (23b) (right)

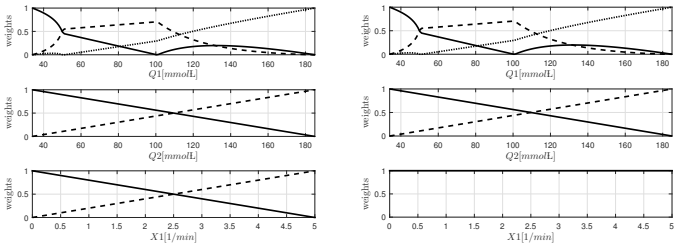

(a) $\mathbf{w}(\mathbf{p}_3)$ (b) $\mathbf{w}(\mathbf{p}_4)$

Figure 2: Weighting functions belong to (23c)

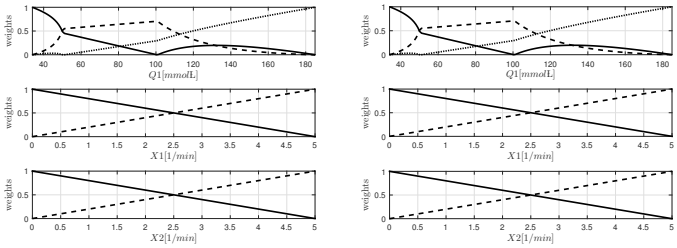

(a) $\mathbf{w}(\mathbf{p}_5)$ (b) $\mathbf{w}(\mathbf{p}_6)$

Figure 3: Weighting functions belong to (23d)

VI. VALIDATION

The "performance" had to be compared for each of our six new TP models to the original nonlinear model. Dense impulse functions were used for the applied CHO and insulin intakes (a10 s10 w5). We aimed to demonstrate that all the realized TP models can approximate the original model even under these unfavorable circumstances, as well. The comparison is based on the $\mathcal{L}_2$ norm of the difference of every TP state vectors $\mathbf{x}_{TP,i}(t)|_{\mathbf{p}_i,i:1,..,6}$ and the corresponding original state vector $\mathbf{x}(t)_{orig}$: $||\mathbf{x}(t)_{orig} - \mathbf{x}_{TP,i}(t)|_{\mathbf{p}_i,i:1,..,6}||_2$. Our goal was to realize all possible TP model variations, which can appropriately mimic the original model. The simple error based comparison for the TP model transformed from the state space form described in (22), where the elements of $\mathbf{T}$ can be seen at the list of possible models enumerated in IV-D.

On Fig. 4 we can see each of the six models compared to the original nonlinear model – the belonging curves totally overlapping with each other. The maximum differences were occurred as the Q_1 and Q_2 states which are loaded with high saturations. The error is around 10^{-4}, which means almost only numerical difference occurred between the realized TP models and the original nonlinear model, respectively. The results are satisfying, concluding that they all TP models represent and approximately mimic the behavior of the original, nonlinear system having moderated error.

VII. CONCLUSION

The study summarized the realization of six TP kind convex polytopic T1DM models via the utilization of the recently developed TP model transformation tool. Some of them have

$$\begin{pmatrix}\Delta\dot{\mathbf{x}}(t)\\ \Delta y(t)\end{pmatrix} = \mathbf{S}\begin{pmatrix}\Delta\mathbf{x}(t)\\ \Delta u(t)\\ \Delta d(t)\end{pmatrix} = \left[\begin{array}{ccccc} \frac{-1}{\tau_D} & 0 & 0 & 0 & 0 \\ \frac{1}{\tau_D} & \frac{-1}{\tau_D} & 0 & 0 & 0 \\ 0 & \frac{1}{\tau_D V_G} & -\left(T_1+\frac{\Delta F(Q_1)}{\Delta Q_1(t)}\right) & k_{12} & 0 \\ 0 & 0 & T_2 & T_3 & 0 \\ 0 & 0 & 0 & 0 & \frac{-1}{\tau_S} \\ 0 & 0 & 0 & 0 & \frac{1}{\tau_S} \\ 0 & 0 & 0 & 0 & 0 \\ 0 & 0 & 0 & 0 & 0 \\ 0 & 0 & 0 & 0 & 0 \\ 0 & 0 & 0 & 0 & 0 \\ 0 & 0 & \frac{1}{V_G} & 0 & 0 \end{array}\right.$$

$$\left.\begin{array}{ccccccc} 0 & 0 & 0 & 0 & 0 & 0 & \frac{1000A_G}{MwG} \\ 0 & 0 & 0 & 0 & 0 & 0 & 0 \\ 0 & 0 & T_4 & 0 & -EGP_0 & 0 & 0 \\ 0 & 0 & T_5 & T_6 & 0 & 0 & 0 \\ 0 & 0 & 0 & 0 & 0 & 1 & 0 \\ \frac{-1}{\tau_S} & 0 & 0 & 0 & 0 & 0 & 0 \\ \frac{1}{\tau_S V_I} & -k_e & 0 & 0 & 0 & 0 & 0 \\ 0 & k_{b1} & -k_{a1} & 0 & 0 & 0 & 0 \\ 0 & k_{b2} & 0 & -k_{a2} & 0 & 0 & 0 \\ 0 & k_{b3} & 0 & 0 & -k_{a3} & 0 & 0 \\ 0 & 0 & 0 & 0 & 0 & 0 & 0 \end{array}\right] \begin{pmatrix}\Delta\mathbf{x}(t)\\ \Delta u(t)\\ \Delta d(t)\end{pmatrix} . \quad (22)$$

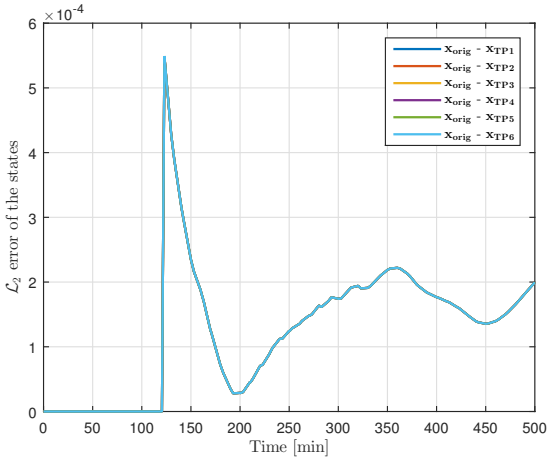

Figure 4: Validation of the TP model

two, others three scheduling parameters (the elements of the parameter vector of the qLPV model). The TP model transformation was executed on every qLPV model. The resulting TP models were separately compared with the original numerical model. In most of the states almost only numerical errors appeared. However, the "core patient model" part contains higher error, which refers rougher approximation. Nevertheless, the order of these errors is around 10^{-4}. Hence, the developed TP model appropriately mimics the original model.

Acknowledgment

The authors thankfully acknowledge the support of the Robotics Special College of Obuda University and the Applied Informatics and Applied Mathematics Doctoral School.

References

[1] P. Baranyi, D. Tikk, Y. Yam, and R. Patton, "TP model transformation as a way to lmi-based controller design," *Comput Ind*, vol. 51, no. 3, pp. 281 – 297, 2003.

[2] P. Baranyi, "TP model transformation as a way to lmi-based controller design," *IEEE T Ind Electron*, vol. 51, no. 2, pp. 387 – 400, 2004.

[3] P. Baranyi, Y. Yam, and P. Varlaki, *Tensor Product Model Transformation in Polytopic Model-Based Control*, 1st ed., ser. Series: Automation and Control Engineering. Boca Raton, USA: CRC Press, 2013.

[4] P. Baranyi, L. Szeidl, P. Várlaki, and Y. Yam, "Definition of the hosvd-based canonical form of polytopic dynamic models," in *3rd International Conference on Mechatronics (ICM 2006)*. ICM, 2006, pp. 660–665.

[5] J. Kuti, P. Galambos, and P. Baranyi, "Minimal volume simplex (mvs) approach for convex hull generation in tp model transformation," in *2014 18th International Conference on Intelligent Engineering Systems (INES 2014)*. IEEE Hungary Section, pp. 187 – 192.

[6] ——, "Minimal volume simplex (mvs) convex hull generation and manipulation methodology for tp model transformation," *Asian J Control*, 2015, submitted.

[7] P. Galambos and P. Baranyi, "TP model transformation: A systematic modelling framework to handle internal time delays in control systems," *Asian J Control*, vol. 17, no. 2, pp. 1 – 11, 2015.

[8] B. Takarics and P. Baranyi, "TP model-based robust stabilization of the 3 degrees-of-freedom aeroelastic wing section," *ACTA Polytech Hung*, vol. 12, no. 1, pp. 209 – 228, 2015.

[9] ——, "Friction compensation in tp model form - aeroelastic wing as an example system," *ACTA Polytech Hung*, vol. 12, no. 4, pp. 127 – 145, 2015.

[10] MTA SZTAKI. (2016) TPtool - Tensor Product MATLAB Toolbox. [Online]. Available: http://tptool.sztaki.hu

[11] R. Hovorka, F. Shojaee-Moradie, P.V. Carroll, L.J. Chassin, I.J. Gowrie, N.C. Jackson, R.S. Tudor, M. Umpleby, and D.H. Jones, "Partitioning glucose distribution/transport, disposal, and endogenous production during ivgtt," *Am J Physiol Endocrinol Metab*, vol. 282, no. 5, pp. E992 – 1007, 2002.

[12] M. Naerum, "Model predictive control for insulin administration in people with type 1 diabetes," Technical University of Denmark, Tech. Rep., 2010.